The United Nations University

GEOTHERMAL TRAINING PROGRAMME
Orkustofnun, Grensásvegur 9,
IS-108 Reykjavík, Iceland

Reports 2004
Number 7

# GEOTHERMAL DISTRICT HEATING AND SWIMMING POOL IN THE SABALAN AREA, IRAN

**Saeid Jalili Nasrabadi**
Renewable Energy Organization of Iran (SUNA)
Yadegare Emam Highway, Poonake Bakhtari Ave., Shahrake Ghods
P.O. Box 14155-6398, Tehran
IRAN
*jalilina@yahoo.com*

**ABSTRACT**

The Sabalan geothermal area in NW-Iran is potentially an important place for tourism in Iran. After realising the plans for building the first geothermal electric power plant in this region and developing swimming pools, using the geothermal water available in this area, hopefully it will be more attractive for tourists and also provide good sanitation facilities for the local people. According to calculations described in the report, Gheynarjeh hot spring has been found to be suitable as a heat source for a swimming pool, both with regard to the required temperature and flow rate. The report also describes the design of a district heating system for Moeil village. The heat load for one sample building was calculated. Comparison of mass flow for a geothermal and fuel-fired system was done, and the influence of radiator size on indoor temperature was analyzed based on a steady-state model. In addition to this, a district heating network was designed and calculations done for it. The simulation results are reasonable and provide a good starting point for a real project.

## 1. INTRODUCTION

Iran has the second largest gas reservoirs in the world and also big oil reservoirs; additionally it has high potential for renewable energy like geothermal, solar, wind, biomass, etc. In 1975, a contract between the Ministry of Energy of Iran (MOEI) and Ente Nazionale per L'Energy Electrica of Italy (ENEL), for geothermal exploration in the north of Iran (Azerbaijan and Damavand regions) was signed. According to the final ENEL reports, priorities should be given to the Sabalan, Damavand, Khoy-Maku and Sahand regions. After the establishment of the Electric Power Research Centre (EPRC) and SUNA (the Renewable Energy Organization of Iran), and after more investigations, the Sabalan region was recommended for the first exploration drilling and electrical generation from geothermal energy in Iran. Hopefully, direct use of geothermal energy will also be established in this area.

Meshkin Shahr is a city in NW-Iran with a population of 164,000. Sabalan Mountain is located southeast of Meshkin Shahr, 4811 m high and at 25 km distance from the city. Meshkin Shahr geothermal prospect lies in the Moil valley on the western slopes of Mt. Sabalan, approximately 16 km

southeast of the Meshkin Shahr city. Mt. Sabalan was previously explored for geothermal resources in 1978, with geological, geochemical and geophysical surveys carried out (Fotouhi, 1995). Renewed interest in the area resulted in further geophysical, geochemical and geological surveys being carried out in 1998. The area includes three geothermal fields located in the northern, eastern and southern parts of the Sabalan central volcano, and a number of geothermal prospects are associated with these (Sahabi et al., 1999). The Meshkin Shahr prospect has been identified as the best of these prospects.

In this paper, two alternatives for direct use of geothermal in the Sabalan geothermal area will be discussed - a swimming pool and a district heating system for the Moeil village. These systems are to be operated in connection with a geothermal power plant for electricity generation that hopefully will be established soon in this area.

## 2. EXPLORATION OF THE MESHKIN SHAHR GEOTHERMAL AREA

### 2.1 Geology

Sabalan is a Quaternary stratovolcano that at present time is at the solfatara stage. Surface geological surveys of the Sabalan area show that most of the area is covered by extrusive rocks (Foutohi, 1995). Mt. Sabalan lies on the south Caspian plate, which underthrusts the Eurasian plate to the north (Bogie et al., 2000). Structurally, the Sabalan area is located in a very complex compressional tectonic zone near the junction of the Eurasian, Iranian and Arabian plates (Bromley et al., 2000). Mt. Sabalan is a large stratovolcano, and consists of an extensive central edifice built on a probable tectonic horst of underlying intrusive and effusive volcanic rocks. The enormous amounts of magma discharged determined the formation of a collapsed caldera about 12 km in diameter, with a depression of about 400 m. The lava flows in the Sabalan are mostly trachy andesite and dacites with alternative explosive phases (Khosrawi, 1996). The schematic geological map (Figure 1) shows the volcanic formations from Eocene to Quaternary.

### 2.2 Geothermal manifestations

There are many geothermal manifestations in the Mt. Sabalan volcanic region; including more than 17 thermal springs. These springs are scattered from the northwest flank to the southeast of Sabalan. The distribution is in groups; Meshkin Shahr, Boushli and Sarein. The average temperature of the thermal springs is about 40°C. The hottest springs are in the Meshkin Shahr group (85°C) and the Boushli group (77°C). The measured maximum flow rate in the Meshkin Shahr group is 9000 l/min and in the Sarein group about 4000 l/min, but there is no record on the Boushli group. Practically all springs display considerably higher flow rate in May than in August (Foutohi, 1995). In Table 1, temperatures, elevations above sea level, mass flows and pH of some of these hot springs have been listed.

TABLE 1: Characteristics of some hot springs in the Meshkin Shahr area (Noorollahi and Yousefi Sahzabi, 2003)

| Location | Temperature (°C) | Elevations (m) | Mass flow (l/s) | pH |
|---|---|---|---|---|
| Moil | 45 | 2200 | 1.5 | 5 |
| Gheynarjeh | 83 | 2120 | 7 | 7 |
| Ilando | 34 | 2010 | 4 | 6 |
| Do-do | 51 | 1990 | 1 | 5 |
| Aghsu | 32 | 2500 | 0.3 | 3 |
| Malek-su | 45 | 2250 | 2 | 6 |

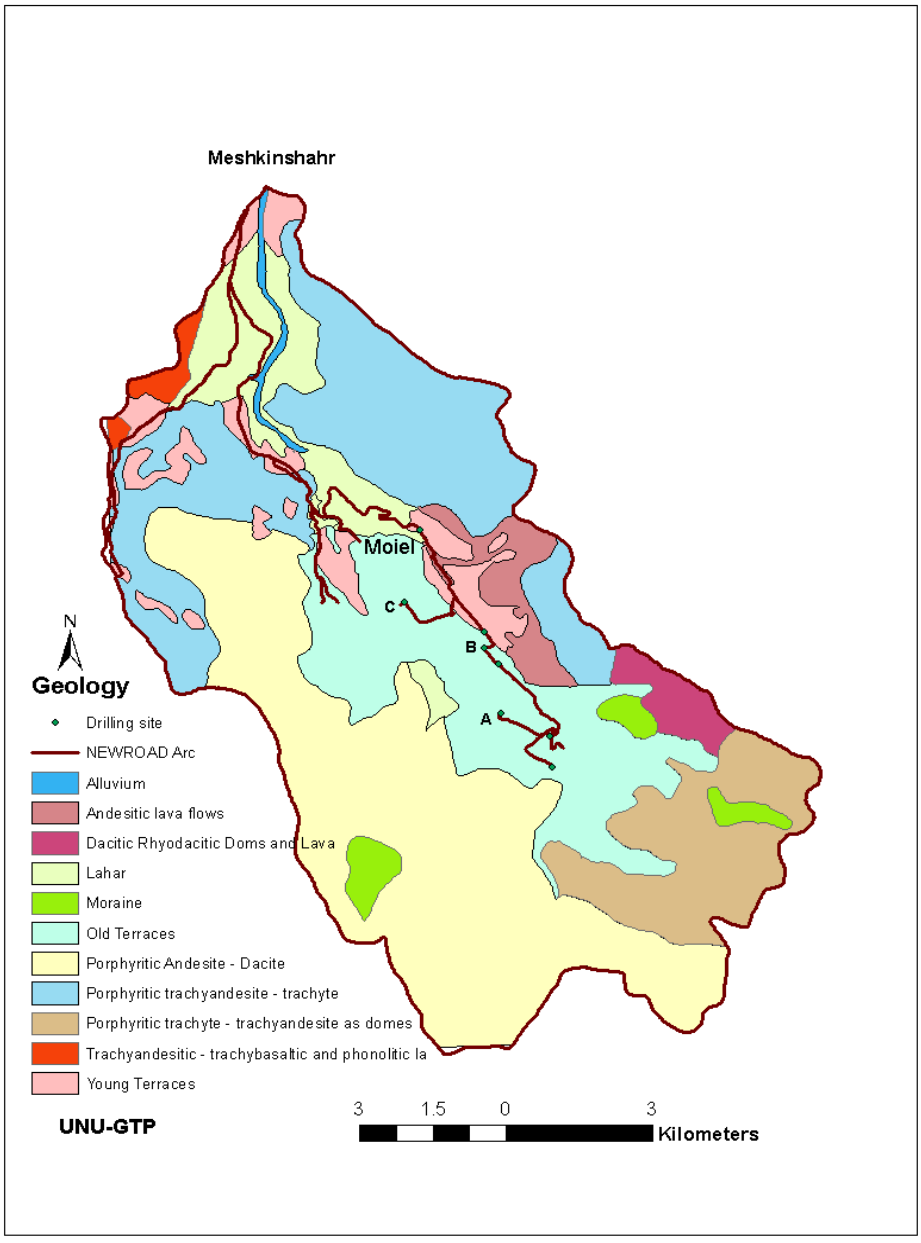


FIGURE 1: Simplified geological map of the Meshkin Shahr area (Yousefi Sahzabi, 2004)

### 2.3 Geochemical exploration

Geochemical studies of the Sabalan region include samples of 65 types of spring waters, 14 gas samples, 30 hydrothermal alteration areas and deposits and 335 samples of run-off waters. The samples were collected from Sarein, Boushli, Meshkin Shahr and Ahar. The main conclusions of the chemistry of the samples taken in the Sabalan area are as follows:

- The thermal water is mixed with ground water. The different degree of mixing and local ground water conditions offset the results of conventional chemical calculation of subsurface condition such as geothermometers.
- The B/Cl ratio in thermal water from Sabalan indicates that the thermal waters in Meshkin Shahr, Boushli and Sarein can have a common source.

- The thermal waters in the Sabalan region originate from a high-temperature geothermal source. Temperatures in excess of 150°C are expected to be found in deep wells.
- The up-flow zone of the Sabalan geothermal system is expected to be found at relatively high elevation and the Meshkin Shahr area is considered the most promising area for exploration drilling (Foutohi, 1995).

### 2.4 Geophysical exploration

During the summer of 1998, a resistivity survey of the Mt. Sabalan geothermal area was undertaken for SUNA. The primary objective of this survey was to carry out geothermal exploration of the Sabalan area to delineate any resistivity anomalies that might be associated with high-temperature geothermal resources. The subsurface resistivity structure was modelled to assess the size of the geothermal resources, to facilitate the choice of initial exploration well sites, and to prepare conceptual models for the hydrology of the geothermal fluid reservoirs. Three complementary resistivity methods were chosen to achieve the desired accuracy and penetration depth range for practical drilling target purposes, DC Schlumberger array for resistivity at shallow depths (10-20 m), TEM method for 20-200 m depth and MT for deeper resistivity, up to 2000 m depth. The results showed large areas of relatively low resistivity (< 5 ohmm), the most significant ones from a geothermal perspective located near the Gheynarjeh/Moeil hot springs and at Sarein, and outlining possible production fields and targets for the first deep exploration wells (Bromley et al., 2000).

### 2.5 Exploration drilling

After the reconnaissance exploration in the Sabalan area, drilling of three exploration wells was planned in the Moeil valley as shown in Figure 2. For drilling these three wells the National Iranian Drilling Company (N.I.D.C.) was selected. SUNA carried out the preparations including civil works as follows:

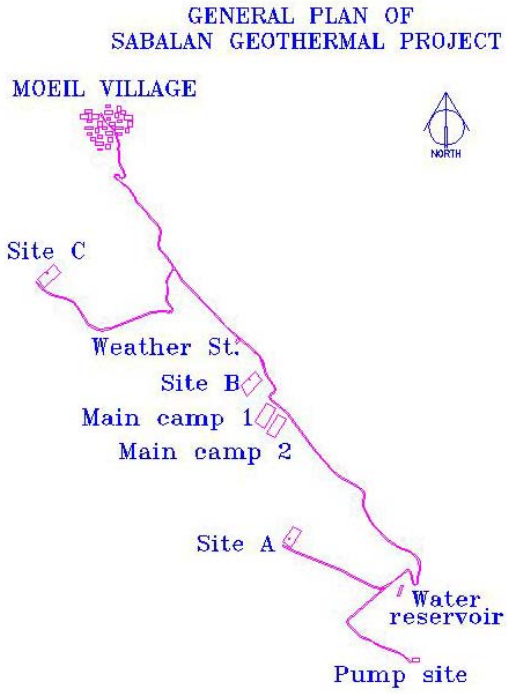


FIGURE 2: Sabalan geothermal project plan with sites of exploration wells

- *Road construction:* About 8 km of new construction and improving about 16 km of an old road from Meshkin Shahr to Moeil village;
- *Construction of drilling sites:* Three drilling sites of 100 × 200 $m^2$ area, named sites A, B and C, were prepared with drilling pad buildings;
- *Water supply for the whole project area:* Building of a pump station, water reservoir with 5000 $m^3$ capacity and laying about 8 km pipelines from pump station to water reservoir and also to each drilling site with 8 inch steel pipes;
- *Camp buildings:* This includes camp for the N.I.D.C.'s staff and workers, and a place for drilling equipment and storage buildings (storage area about 2000 $m^2$);
- *Weather station:* Building used as an information centre and also office for SUNA's staff.

Drilling of the first geothermal exploration well (Site A) west of Mt. Sabalan started in November 2002, and the third exploration well (Site B) was finished in May 2004. Table 2 shows more information about the five wells drilled in this project (including shallow re-injection wells).

TABLE 2: Properties and present status for the wells drilled in the Sabalan geothermal field

| No. | Site | Well name | Depth (m) | Present status |
|---|---|---|---|---|
| 1 | Site A | NWS-1 | 3197 | Discharge test in May 2004; well head pressure 3.5 bar, well produces 40 kg/s of two-phase fluid at temperature of < 200°C. |
| | | NWS-2 | 652 | Re-injection well for NWS-1. |
| 2 | Site B | NWS-4 | 2265 | Water level at 114 m, $T_{max}$=223°C at 2010 m, P=2366 psi - during the writing of this report, this well was going to be tested. |
| | | NWS-5 | 494 | Re-injection well for NWS-4. |
| 3 | Site C | NWS-3 | 3170 | Water level at 15 m, $T_{max}$=148°C at 2600 m, P=3315 psi. |

## 3. SWIMMING POOL IN THE SABALAN GEOTHERMAL AREA, MESHKIN SHAHR

Swimming has been one of the favourite sports in Iran for many years. Also, based on religion and cultural background, swimming is very important from the point of sanitation. Public baths have existed in most parts of Iran for many years. Coal, wood, oil, etc. are used for heating the water. In almost all areas where hot springs are found, the geothermal water is used for pools for bathing, mainly because of therapeutic effects but also for relaxation. In present time, especially in the Meshkin Shahr and Sarein cities (NW-Iran), there are many swimming pools using geothermal water directly. In this part of the paper the design of a swimming pool for the Moeil village by using geothermal water as a heat source will be discussed.

### 3.1 Size of the swimming pool

The size of a swimming pool is one of the important items for design of the pool; it is a basic factor for determining the pool's service, water value, selection of equipment etc. Here swimming pools are being built for students who are learning to swim, people who swim for sport and their relaxation, and for tourists.

The swimming area of a pool should be based on 3.5 $m^2$ per swimmer. For proper swimming, a lane at least 2.0 m wide and 5.0 m long is required. The designer feels that in a pool which is intended only for swimming, and not for diving and water polo, the maximum depth of water need not to exceed about 1.5 m. For the teaching part of a swimming pool, the amateur swimming association recommends a minimum length of 12.0 m and a minimum width of 7.0 m. The depth generally varies from 0.8 m to 1.0 m. The maximum depth should not exceed 1.2 m (Perkins, 1988). Further, it is assumed that the maximum number of swimmers in the pool at the same time will be 60. Thus, the required surface area is 210 $m^2$, which is the minimum requirement according to standards.

The pool shall have two parts, one part of the size 25 × 13 m with the depth 1 m in the shallow end and 1.8 m in the deep end. The second part is to be a teaching pool of the size 12.5 × 7 m with the depth 0.75 m in the shallow end and 0.90 m in the deep end of the pool. Thus the total water volume of the pool needs to be 527.2 $m^3$ and the total pool area is calculated as 412.5 $m^2$.

### 3.2 Schematic diagram of the swimming pool

Figure 3 shows a schematic diagram of the swimming pool. The method adopted for distributing the purified water to the pool and the withdrawal of the contaminated water is of the utmost importance in maintaining the whole of the water in the pool at the required standard of purity and temperature if the water is heated.

A balancing tank is required to even out variations in the quantity of water leaving and entering the pool. A reasonable basis for calculation of the size of the balancing tank is the following:

1. 70 litres per swimmer for the estimated maximum number of customers;
2. Quantity of water required to back-wash one filter;
3. To the total of 1 and 2 add 10% to cover overflow from the pool due to wave action.

The total of 1, 2 and 3 gives the net capacity of the balancing tank (Perkins, 1988).

The oldest and most popular method of filtration is sand. Sand filters share two things in common:

1. When in the filtration mode, water always flows from top to bottom;
2. All of them have some sort of lateral or under drain with slots to hold back sand while allowing clean, filtered water to pass through.

The sand filters use special filter sand, normally 0.45-0.55 mm, which has sharp edges that serve to separate particles, allowing filtration to take place. They operate on the basis of "depth" filtration; dirt is driven through the sand bed and trapped in the minute spaces between the particles of sand. Initially, a clean sand bed will remove larger particles, and then, as the bed starts to load up with dirt, it will remove finer particles. Cleaning of the media, or sand, is accomplished through reversing the flow through the filter, to the "waste" line. This is known as backwashing.

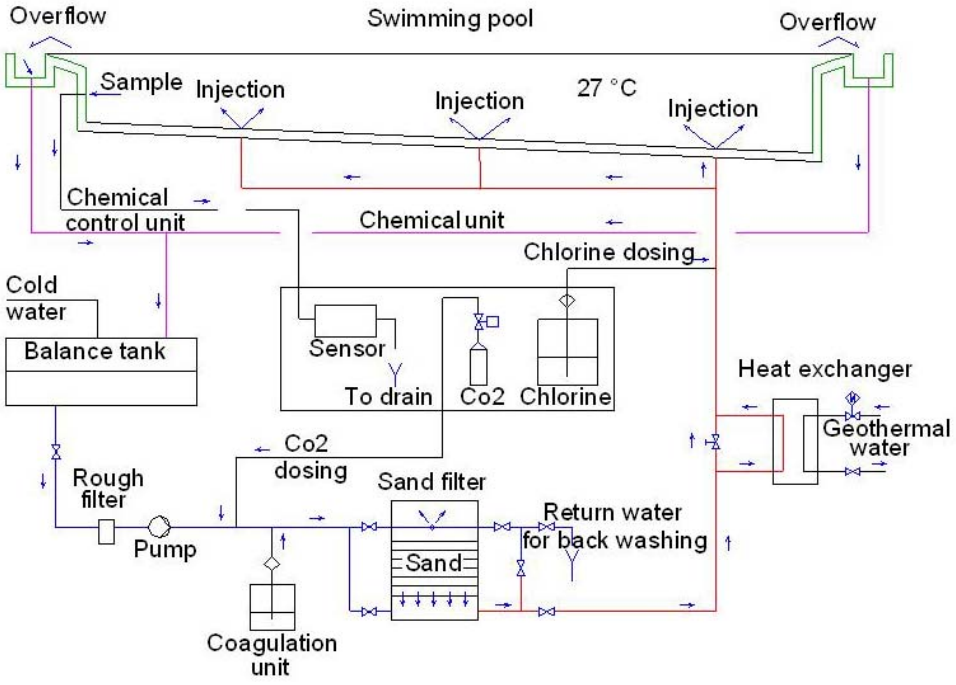


FIGURE 3: A schematic view of the swimming pool

The rough filter is working as protection equipment for the circulating pump by removing large impurities like sand particles, hairs, etc. It increases the lifetime of the impellers of the pump and decreases the requirement for the back washing process in the filter sand.

A chemical control unit controls the concentration of chemicals in the system. As shown in Figure 3, samples are taken directly from the pool's water. When there are any changes identified in chemical properties, the sensor will send an electrical signal to improve chemical compounds in the pool's water.

Coagulation and flocculation of microorganisms is of practical importance in waste water treatment because flocculated organisms are relatively easy to collect from the various streams in a wastewater treatment plant. Chemical coagulation of biologically treated wastewaters is usually the initial step in water renovation systems. Coagulants used today generally consist of alum, lime or a synthetic polyelectrolyte. Separation of the floc is accomplished by flotation or sedimentation (Rensselaer, 2004).

### 3.3 Water circulation in the pool

The turnover period is one of the most important factors in operation of the swimming pool. It is the time it takes to circulate all the water in the pool through all the outlets and inlets and all circulation lanes. It changes with the pool loading and mostly depends on the type of pool. For the teaching part of the pool, the turnover period is defined as 1.5 hours and for the other part of the pool 4 hours according to standards (Perkins, 1988). For maintenance of water quality, at least 2 $m^3$ of properly treated water should be returned to the pool each day for each bather.

Using chlorine is the proven way to destroy bacteria, viruses and alga in the pools. A Clearwater Chlorinator produces its own chlorine when mildly salted water is passed through the Salt Cell (salt is made up of two elements- sodium and chlorine). The chlorine dissolves instantly in the water, going to work immediately to safely sanitize. A Clearwater Chlorinator also produces a small amount of ozone which gives that added sparkle and freshness. The Salt Cell is simply fitted to the plumbing between the filter and water outlet and the Control Unit is mounted adjacent to the Cell for easy monitoring and control. Clearwater systems are designed to handle the lowest concentration levels of salt in water and cope with enormous variations in salinity, from a minimum of 3,000 ppm up to seawater levels of 35,000 ppm. Three important factors influence which Clearwater model should be chosen, size, number of bathers per day and climatic conditions. Daily operation of the chlorination and filtration system will vary during unusually hot periods or heavy bather loads requiring longer running of the system. By choosing the right Clearwater model to cope with these factors, the filtration system running times can be minimized saving further costs (Pool Warehouse, 2004).

### 3.4 The piping system of the swimming pool

Water conveyance, water treatment, and in fact the entire swimming pool technology requires pipes and piping system components in large numbers. The selection of materials plays an important role for the water quality of the entire operation and its service life. Thermal water has curative properties, but it can also be very aggressive. All pipes made of polypropylene (PP) or polyethylene (PVC) have passed the tests, so the pipe material chosen is PVC and PP which can resist the above conditions. Before concreting of the floor, pipes with large diameter must be put in the bottom. It will provide good facility for the pipes so they can be connected and packed later. Also, if there are problems with the pipes during operation, they can be solved without any destruction of the walls or floor of the pool.

The water distribution system in the swimming pool is accomplished with the piping system. The turnover period is the main factor for determining the piping system properties and the amount of mass

flow through the pipes in the bottom of the pool. Calculation of mass flow through each inlet nozzle in the floor of the pool is shown below:

For the public and teaching parts of the swimming pool with size as defined in Section 3.2, the water volume can be calculated with Equation 1:

$$V = LW\frac{d_1 + d_2}{2} \tag{1}$$

where $V$ = Water volume ($m^3$);
$L$ = Length (m);
$W$ = Width (m);
$d_1$, $d_2$ = Minimum and maximum depth of pool (m).

For the public part of the swimming pool, the volume is: $V_{public} = 455\ m^3$

For the teaching part of the swimming pool, the volume is: $V_{teaching} = 72.2\ m^3$

With turnover periods equal to 4 and 1.5 hours for the public and teaching parts of the pool, respectively, the amount of mass flow can be calculated as:

$$m = \frac{V}{T_o}$$

where $m$ = Mass flow (l/s);
$T_o$ = Turnover period (hour).

For the public part of the swimming pool the mass flow is: $m_{public} = 455/4 = 113.75\ m^3/hr = 31.6$ l/s.

For the teaching part of the swimming pool the mass flow is: $m_{teaching} = 72/1.5 = 48\ m^3/hr = 13.3$ l/s.

From the number of inlet nozzles in the floor of the pool (Figure 4), the mass flow through each of them can be calculated as:

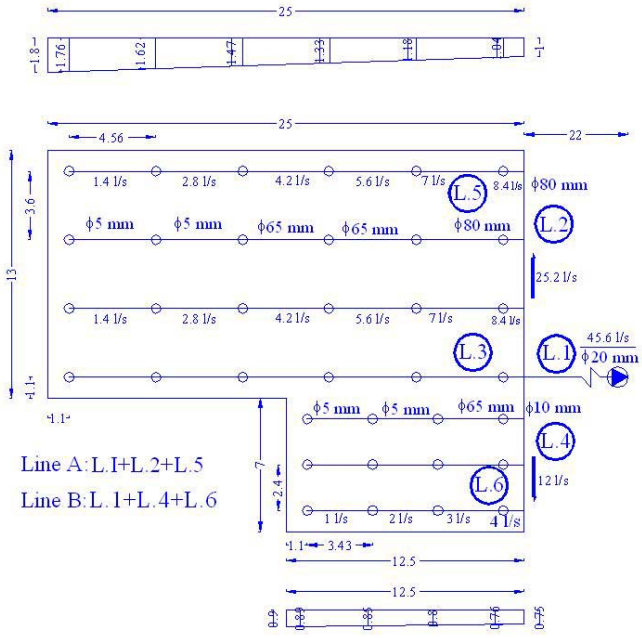


FIGURE 4: Overview of the pipeline layout

$$m_{in} = \frac{m}{n_o}$$

where $m_{in}$ = Mass flow through each inlet nozzle;
$n_o$ = No. inlet nozzles in the bottom of pool.

Public part of swimming pool:
$m_{in} = 31.6/24 \approx 1.4$ l/s / inlet nozzle

Teaching part of swimming pool:
$m_{in} = 13.3/12 \approx 1.1$ l/s / inlet nozzle

Based on these calculations and the pressure drop in the whole system (see Section 3.5) the diameter of pipes can be selected. Figure 4 shows the water distribution system, pipe diameters and water flow in each pipe section in the pool's floor.

### 3.5 Pressure drop calculation and pump selection

Based on the maximum flow rate and pressure drop in the water circulation system, circulation pumps can be selected. Maximum flow rate has been calculated in Section 3.4 from the turnover time, and it is 44.9 l/s. One way of calculating the pressure drop in the pipelines is using Equation 2 (Olson, 1973), assuming an appropriate value for the roughness factor, *k*:

$$\Delta P = \frac{\rho v^2}{2} \frac{fL}{D} \tag{2}$$

where: $\Delta P$ = Pressure drop (kPa);
$f$ = $1/ (2 \log D/2k + 1.74)^2$;
$k$ = Roughness factor;
$\rho$ = Density of fluid (kg/m$^3$);
$v$ = Velocity of fluid (m/s);
$L$ = Length of pipe (m);
$D$ = Diameter of pipe (m).

Here another approach has been used, based on the pressure drop diagram in Figure 5. From Figure 4, it can be seen that there are two flow paths that are candidates for the critical path in the system with regard to pressure drop, lines A and B. The pressure drop must be calculated in both of them and thereafter compared to find the maximum pressure drop in the system. The pressure drop diagram has been used to find the pressure drop and water velocity in lines A and B according to the mass flow through each pipe section and pipe diameter. The pressure drop in lines A and B was found to be 24.15 kPa and 15.68 kPa, respectively (Table 3). This means that line A is the critical line with 24.15 kPa pressure drop.

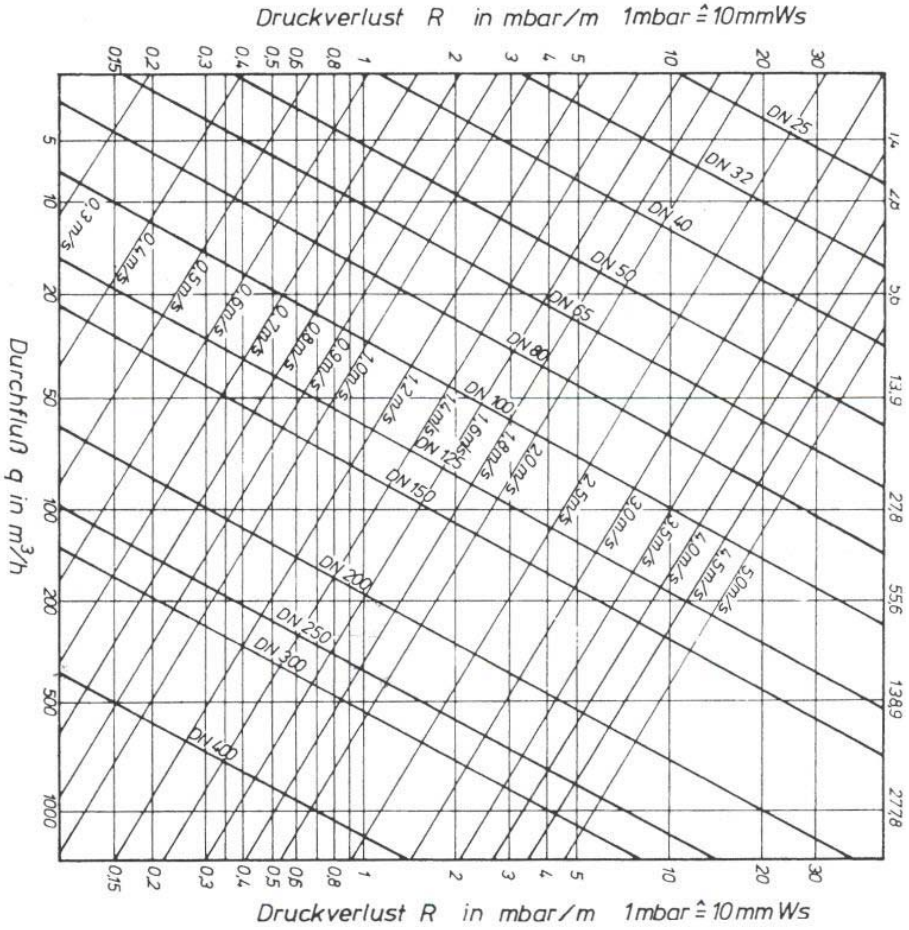


FIGURE 5: Pipe manufactory catalogue for pressure drop calculation

TABLE 3: Pressure drop calculation in the two critical lines A and B

| **Pressure drop in the system from pump to pool in line A** | | | | | | | | | | |
|---|---|---|---|---|---|---|---|---|---|---|
| **Velocity (m/s)** | **Flow rate (l/s)** | **Length (m)** | **dp for k=1, v (kPa)** | **k** | **No. of bends** | **dp at v in bend (kPa)** | **Pipe diameter (m)** | **dp (mbar/m)** | **dp (kPa/m)** | **dp in pipe (kPa)** |
| 1.36 | 8.40 | 1.10 | 9.28 | 1.30 | 1.00 | 1.21 | 0.08 | 2.36 | 0.24 | 0.26 |
| 1.20 | 7.00 | 4.56 | 7.20 | 1.30 | 1.00 | 0.94 | 0.08 | 1.87 | 0.19 | 0.85 |
| 1.50 | 5.60 | 4.56 | 11.30 | 1.30 | 1.00 | 1.47 | 0.065 | 3.40 | 0.34 | 1.55 |
| 1.08 | 4.20 | 4.56 | 5.88 | 1.30 | 1.00 | 0.76 | 0.065 | 1.87 | 0.19 | 0.85 |
| 1.08 | 2.80 | 4.56 | 5.88 | 1.30 | 1.00 | 0.76 | 0.05 | 2.36 | 0.24 | 1.08 |
| 0.64 | 1.40 | 4.56 | 2.08 | 0.50 | 1.00 | 0.10 | 0.05 | 0.90 | 0.09 | 0.41 |
| 1.36 | 8.40 | 3.60 | 9.28 | 0.50 | 1.00 | 0.46 | 0.08 | 2.36 | 0.24 | 0.85 |
| 1.10 | 16.80 | 3.60 | 6.10 | 1.30 | 1.00 | 0.79 | 0.13 | 0.90 | 0.09 | 0.32 |
| 1.30 | 25.20 | 3.60 | 8.50 | 1.30 | 1.00 | 1.11 | 0.15 | 1.38 | 0.14 | 0.50 |
| 1.36 | 45.60 | 22.00 | 9.28 | 1.50 | 2.00 | 2.78 | 0.20 | 0.77 | 0.08 | 1.69 |
| **Pressure drop in the system from pool to pump** | | | | | | | | | | |
| 1.36 | 45.60 | 40.00 | 9.28 | 0.50 | 5.00 | 2.32 | 0.20 | 0.77 | 0.08 | 3.08 |
| | | | | | | 12.71 | | | | 11.44 |
| **Total pressure drop in line A** | | | | | | | | | | **24.15** |

| **Pressure drop in the system from pump to pool in line B** | | | | | | | | | | |
|---|---|---|---|---|---|---|---|---|---|---|
| **Velocity (m/s)** | **Flow rate (l/s)** | **L (m)** | **dp for k=1, v (kPa)** | **k** | **No. of bends** | **dp at v in bend (kPa)** | **Pipe diameter (m)** | **dp (mbar/m)** | **dp (kPa/m)** | **dp in pipe (kPa)** |
| 0.60 | 1.00 | 3.43 | 1.80 | 0.50 | 1.00 | 0.09 | 0.05 | 0.80 | 0.08 | 0.27 |
| 0.90 | 2.00 | 3.43 | 4.10 | 1.30 | 1.00 | 0.53 | 0.05 | 1.71 | 0.17 | 0.59 |
| 0.80 | 3.00 | 3.43 | 3.20 | 1.30 | 1.00 | 0.42 | 0.065 | 1.13 | 0.11 | 0.39 |
| 1.00 | 4.00 | 1.10 | 5.00 | 1.30 | 1.00 | 0.65 | 0.065 | 1.70 | 0.17 | 0.19 |
| 1.00 | 4.00 | 2.40 | 1.05 | 0.50 | 1.00 | 0.05 | 0.065 | 1.70 | 0.17 | 0.41 |
| 0.90 | 8.00 | 2.40 | 4.10 | 1.30 | 1.00 | 0.53 | 0.10 | 0.85 | 0.09 | 0.20 |
| 1.30 | 12.00 | 2.20 | 8.50 | 1.30 | 1.00 | 1.11 | 0.10 | 1.70 | 0.17 | 0.37 |
| 1.36 | 45.60 | 22.00 | 9.28 | 1.50 | 2.00 | 2.78 | 0.20 | 0.77 | 0.08 | 1.69 |
| **Pressure drop in the system from pool to pump** | | | | | | | | | | |
| 1.36 | 45.60 | 40.00 | 9.28 | 0.50 | 5.00 | 2.32 | 0.20 | 0.77 | 0.08 | 3.08 |
| | | | | | | 8.48 | | | | 7.19 |
| **Total pressure drop in line B** | | | | | | | | | | **15.68** |

Table 4 shows pressure drop for the heat exchanger and sand filter. These have not been calculated, but have been selected according to experimental and recommended values through the manufacturers, consultants and consumers.

A circulation pump must be selected according to the calculated flow rate and total pressure drop in the system, plus a safety margin of 20%. Thus, the selection is based on the flow rate of 46 l/s and a pressure drop equal to 132 kPa. This has been done through an Internet site from the Alfa Laval manufacturers with properties as shown in Table 5 (Pump-flo.com, 2004). Figure 6 shows the selected pump's curve.

TABLE 4: Pressure drop in the whole system

| No. | Pressure drop in different parts of the system | Pressure drop (kPa) |
|---|---|---|
| 1 | Heat exchanger | 15 |
| 2 | Sand filter | 50 |
| 3 | Different elevation of pump and pool | 20 |
| 4 | Pressure drop in the water lane according to calculations in Table 3 | 25 |
| | Total pressure drop in the whole system | 110 |

TABLE 5: Properties of selected circulation pump for the swimming pool

| Properties | Value |
|---|---|
| Type and size | C4410x4.0x4.0x10 |
| Rotational speed (rpm) | 1450 rpm |
| Head (m) | 13.8 |
| Efficiency at specified flow rate | 65% |
| NPSH required by pump manufacturer at specif. flow rate (m) | 3.36 |
| Power (kW) | 9.29 |
| Engineering units | metric |
| Synchronous speed (Hz) | 50 |

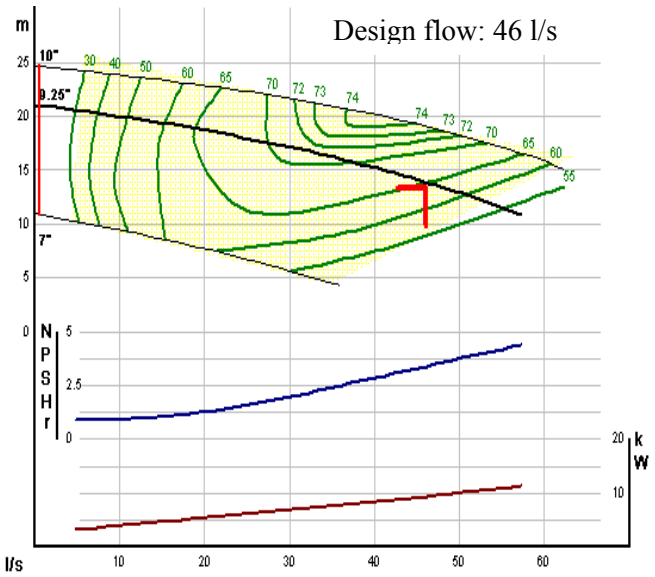


FIGURE 6: Selected circulation pump's curve

### 3.6 Heat loss from the pool

Heat loss from outdoor pools is mainly due to (Svavarsson, 1990):

- Convection
- Evaporation
- Radiation
- Conduction
- Rain

The main heat losses from the swimming pool occur by convection and evaporation. The obtained results from earlier research and analyses show that heat losses due to the other three factors (radiation, conduction, rain) can be estimated to be equal to 10% of total heat loss due to convection and evaporation. Heat loss due to conduction is small, because of good insulation in the pool building materials. Heat loss by means of rain and radiation is also not very big. In the following calculation, 10% of total heat loss by convection and evaporation will be assumed for these three mentioned factors.

**Heat loss due to convection:** Heat loss due to convection depends strongly on the air temperature around the pool and the wind speed. Equation 3 shows that heat loss through convection will increase with higher wind speed and lower outside temperature:

$$q_C = h_c(T_w - T_a) \tag{3}$$

where $q_c$ = Amount of heat loss by convection (W/m$^2$);
$T_w$ = Water temperature in the pool (°C);
$T_a$ = Air temperature in the pool's surroundings (°C);
$h_c$ = Convection heat transfer coefficient (W/m$^2$°C), is very dependent on wind speed.

The relationship between heat transfer coefficient and wind speed is shown in Equation 4 that is called the Rimsha-Doncenko formula:

$$h_c = 4.19(k + 0.45v) \tag{4}$$

where $v$ = Wind speed at 2 m height from the ground surface (m/s);
$k$ = Empirical coefficient (W/m$^2$°C) defined by Equation 5.

$$k = 0.93 + 0.04(T_w - T_a) \tag{5}$$

**Heat loss due to evaporation:** Heat loss due to evaporation takes place when there is different partial pressure of water vapour at the pool's surface and in the air over the pool. This will cause evaporation of water at the pool surface, and this requires energy that is taken from the water. This kind of heat loss in the pool can be calculated with Equation 6 from Rimsha – Doncenko (Svavarsson, 1990):

$$q_E = 4.19(1.56k + 0.70v)(e_W - e_a) \tag{6}$$

where $q_E$ = Amount of heat loss by evaporation (W/m$^2$);
$e_W$ = Partial pressure of steam at surface (mbar);
$e_a$ = Partial pressure of steam in the air above the pool (mbar).

The total heat loss can thus be calculated as:

$$q_T = q_E + q_C + S \tag{7}$$

where $q_T$ = Total heat loss from the swimming pool (W/m$^2$);
$S$ = Sum of heat losses due to radiation, conduction and rain = 0.1 ($q_E$ + $q_C$) (W/m$^2$).

Both input and calculated parameters are shown in Table 6.

The final result is that the total heat loss from the pool is: $q_T$ = 711 kW.

### 3.7 Energy requirement for heating the pool

The total heat loss from the swimming pool has been calculated and the same quantity of heat must be added to the water supplied to the pool. This is done through a heat exchanger that transfers heat from geothermal water to fresh water that is used as pool water, or:

$$q_T = q_i \tag{8}$$

where $q_i$ = Required quantity of heat for the pool (W/m$^2$).

Equation 9 (Wark, 1988) is used for calculation of the amount of geothermal water needed as a heat source and the temperature of the pool's heated water by a heat exchanger. It is known as the energy balance equation in the steady-flow condition.

$$Q_i = m_1 c_{p1}(T_2 - T_1) = m_2 c_{p2}(T_3 - T_4) \quad (9)$$

where $m_1$ = Amount of water required for circulation in the system (kg/s);
$m_2$ = Amount of geothermal water as a heat source (kg/s);
$c_p$ = Specific heat capacity of water (J/kg°C);
$T_1$ = Temperature of pool's cold water before heated by heat exchanger (°C);
$T_2$ = Temperature of pool's heated water by heat exchanger (°C);
$T_3$ = Temperature of inlet geothermal water at heat exchanger (°C);
$T_4$ = Temperature of outlet geothermal water at heat exchanger (°C);
$Q_i$ = Amount of required heat for the pool (W).

The results are $m_2$ = 4.25 l/s and $T_2$ = 30.7°C.

Table 6 shows all input and calculated parameters in the calculation of the required heat for the pool, the geothermal water's flow rate, pool water temperature after heat exchanger and the total heat loss from the swimming pool.

TABLE 6: Parameters for heat loss and energy requirements in the swimming pool

| **Known factors - design conditions** | **Parameter** | **Value** | **Unit** |
|---|---|---|---|
| Air temperature | $T_a$ | -5 | °C |
| Wind speed | $v$ | 5 | m/s |
| Humidity (max) | H | 60 | % |
| Amount of required water for circulation in the system | $m_1$ | 45.6 | l/s |
| Specific heat capacity of water | $c_p$ | 4.18 | kJ/kg°C |
| Temperature of pool's cold water before heated by heat exchanger | $T_1$ | 27 | °C |
| Temperature of inlet geothermal water at heat exchanger | $T_3$ | 75 | °C |
| Temperature of outlet geothermal water at heat exchanger | $T_4$ | 35 | °C |
| Pool's area | $A$ | 413 | $m^2$ |
| **Calculated values** | | | |
| Amount of required heat for the pool | $Q_i$ | 711 | kW |
| Amount of geothermal water as a heat source | $m_2$ | 4.25 | l/s |
| Temperature of pool's heated water by heat exchanger | $T_2$ | 30.7 | °C |
| Coefficient depending on temperature difference | $k$ | 9.25 | $W/m^2°C$ |
| Heat transfer coefficient | $h_C$ | 18.7 | $W/m^2°C$ |
| Convectional heat loss | $q_c$ | 598 | $W/m^2$ |
| Partial pressure of steam at water surface | $e_w$ | 35.7 | mbar |
| Partial pressure of steam in the air above the pool | $e_a$ | 2.41 | mbar |
| Amount of heat loss by convection | $q_E$ | 968 | $W/m^2$ |
| Total heat loss from the swimming pool | $q_T$ | 1723 | $W/m^2$ |

### 3.8 Selection of heat exchangers

Based on the input data and calculated results from Table 6, a suitable heat exchanger can be ordered from manufacturers.

## 4. DISTRICT HEATING FOR MOEIL VILLAGE

Moeil village is the nearest place to Sabalan geothermal field as shown in Figure 2. According to the weather conditions in this area, space heating for Moeil is an important project. Presently, oil is used for space heating. In this part of the report, a district heating system for Moeil will be discussed.

### 4.1 Weather conditions

Analysis of the outdoor temperature in the area being surveyed is the first step for district heating system design and simulation.

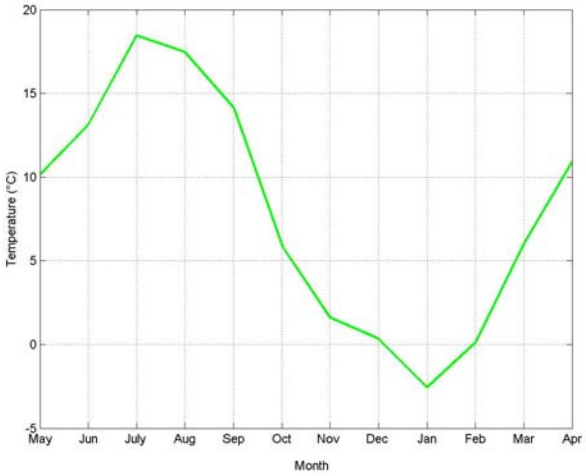


FIGURE 7: Monthly average outdoor temperature (°C)

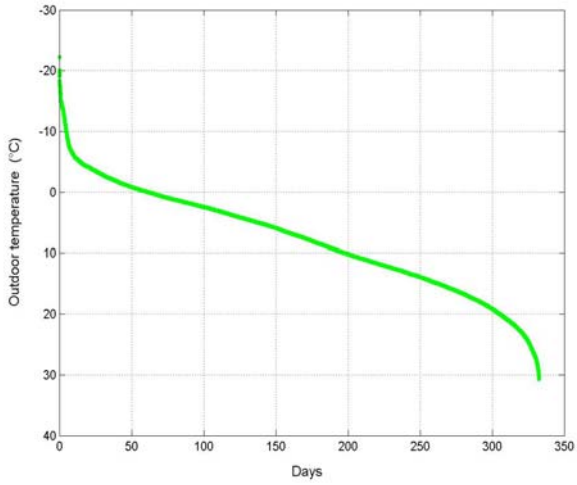


FIGURE 8: Duration curve of outdoor temperature

Figure 7 shows the measured monthly average outdoor temperature from May 2000 to April 2001 in the Moeil village. The maximum and minimum temperatures are about 30°C and -22°C in July and January, respectively. The annual average temperature is about 7°C. Figure 8 shows the duration curve of outdoor temperature in this area.

### 4.2 Heat transfer in buildings

In order to calculate the heat load in buildings, the relationship between the building and its surroundings must be defined. Heat transfer is a transient flow of thermal energy from one system to another due to temperature difference between two systems. There are three kinds of heat transfer: conduction, convection and radiation. In most cases, heat transfer is dominated by conduction and convection.

#### 4.2.1 Heat transfer calculations

When systems are in physical contact, heat transfer will happen in conduction mode. This transient will be from the hotter molecule to the cooler molecule. Heat transfer rate, $q_c$ per unit area, $A$, is proportional to the normal temperature gradient. Thus:

$$\frac{q_c}{A} \sim \frac{\Delta T}{\Delta x} \tag{10}$$

or Fourier's law, as follows:

$$q_c = -kA\frac{dT}{dx} \tag{11}$$

Equation 11 can be simplified by assuming that heat transfer is in a homogeneous material and, $k$ is constant. So the following equation is reached:

$$\frac{q_C}{A} = \frac{k}{\Delta x}(T_1 - T_2) \tag{12}$$

where $\Delta x$ = The thickness separating the surfaces, which are at $T_1$ and $T_2$.

By rearranging Equation 12, the following relation is obtained:

$$\frac{q_C}{A} = \frac{(T_1 - T_2)}{\Delta x / k} = \frac{T_1 - T_2}{R_C} \tag{13}$$

where $R_C$ = The thermal resistance due to conduction ($m^2°C/W$).

$R_C$ is defined as follows:

$$R_C = \Delta x / k \tag{14}$$

For one composite wall made of different layers and number of materials (Figure 9), the following relationship can be obtained, knowing that the heat flow is the same in each of the layers, thus:

$$q_c = q_{c1} = q_{c2} = q_{c3} \tag{15}$$

$$q_c = \frac{T_1 - T_2}{\Delta x_1 / k_1 A} = \frac{T_2 - T_3}{\Delta x_2 / k_2 A} = \frac{T_3 - T_4}{\Delta x_3 / k_3 A} \tag{16}$$

By solving Equation 16, it can be concluded that:

$$\frac{q_c}{A} = \frac{T_1 - T_4}{\Delta x_1 / k_1 + \Delta x_2 / k_2 + \Delta x_3 / k_3} \tag{17}$$

or

$$\frac{q_c}{A} = \frac{T_1 - T_4}{R_1 + R_2 + R_3} \tag{18}$$

$$\frac{q_c}{A} = \frac{T_i - T_o}{R_o + R_1 + R_2 + R_3 + R_i} \tag{19}$$

where $R_o$ and $R_i$ = Outside and inside film thermal resistances of the fluid, respectively.

Therefore, the total thermal resistance of heat transfer is given as follows:

$$R = R_o + \sum_{k=1}^{n} R_k + R_i \tag{20}$$

where $n$ = Total number of layers of the composite wall.

The overall heat transfer coefficient of the wall is defined as follows:

$$U = \frac{1}{R} \tag{21}$$

Therefore, the heat transfer from the building to the environment can be calculated according to the following:

$$q_c = UA(T_i - T_o) \tag{22}$$

where $T_i$ and $T_o$ = Inside and outside design temperature, respectively (°C).

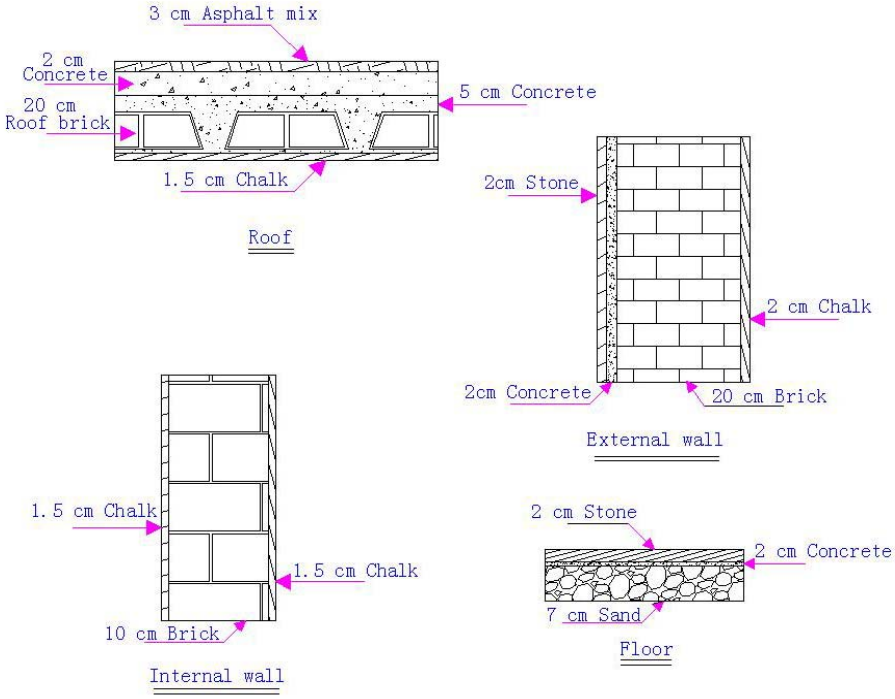


FIGURE 9: Building surfaces construction layouts

### 4.2.2 Convection heat transfer

When heat is transferred between two systems by means of a moving fluid such as air or water, it is referred to as convection heat transfer. There are two types: forced convection, and free convection. Newton's law of cooling given in the following equation, is the general equation for heat transfer by convection:

$$q_h = hA(T_w - T_o) \tag{23}$$

where $h$ = Convection heat transfer coefficient (W/m$^2$°C), the value depends on the complexity of the system;
$A$ = Heat transfer surface area (m$^2$);
$T_w$ = Wall surface temperature (°C);
$T_o$ = Air temperature (°C).

Equation 23 can also be rearranged as follows:

$$q_h = \frac{T_w - T_o}{1/hA} = \frac{T_w - T_o}{R_{conv}} \tag{24}$$

where $R_{conv}$ = $1/hA$ = The thermal resistance due to convection heat transfer.

### 4.2.3 Radiation heat transfer

Heat transfer by conduction and convection requires a medium for existence. Heat transfer by radiation can take place in a vacuum, and it is an electromagnetic radiation. The net heat exchange by radiation from an object to isothermal surroundings is given by the following equation:

$$q_r = \sigma A_1 \varepsilon (T_1^4 - T_2^4) \tag{25}$$

where $q_r$ = Rate of heat transfer by radiation (W);
$\sigma$ = Stefan-Boltzman constant = $5.669 \times 10^{-8}$ W/m$^2$K$^4$;
$A_1, A_2$ = Area of surface 1 and surface 2, respectively (m$^2$);
$\varepsilon$ = Common emissivity of the object;
$T_1, T_2$ = Temperatures of surface 1 and the surroundings, respectively (°C).

### 4.3 Building calculations

There are two kinds of common buildings in the Meshkin Shahr city. In the old part of city, the buildings have at least two stories but without any heat insulation. In the new part of city, the buildings are with four or five stories and with good heat storage capacity.

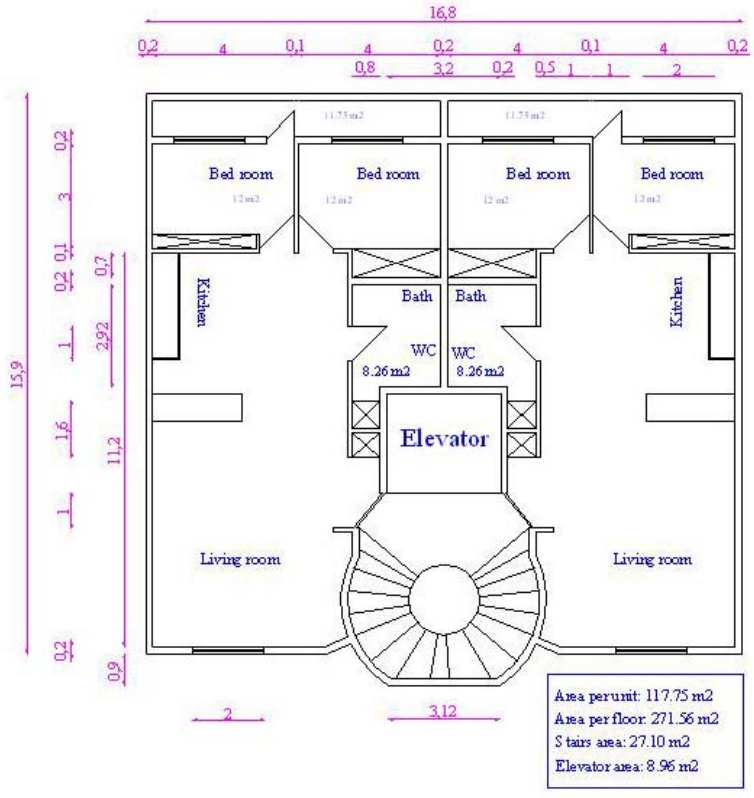


FIGURE 10: Selected sample building's plan and details

Building heating systems in the Moeil village are not standard in view of its structure and energy storage, so new buildings close to Moeil village that are expected to be built following the building of the first geothermal electric power plant will be discussed. A sample building with four stories is shown in Figure 10. The reference outdoor temperature is -5°C and indoor temperature is 20°C. It has single glass windows and wooden doors.

### 4.3.1 Construction material

For calculation of building parameters, construction material properties must be defined (Emeish, 2001). The building is divided into external walls, roof, floor and internal walls. Table 7 shows the construction material of these surfaces and their thermal properties.

TABLE 7: Thermal properties of construction material

| Construction material | Density ($kg/m^3$) | Thermal conductivity (W/m°C) | Heat capacity (kJ/kg°C) |
|---|---|---|---|
| Concrete | 2088 | 1.21 | 1.08 |
| Brick | 1800 | 0.6 | 1.80 |
| Chalk | 2710 | 4.64 | 0.86 |
| Asphalt mix | 2000 | 0.70 | - |
| Roof bricks | 1400 | 0.95 | 1.08 |
| Sand | 1450 | 0.38 | 0.92 |
| Cement tiles | 2145 | 1.35 | 0.96 |
| Stone | 2580 | 2.27 | 0.88 |

Table 8 shows the total area of roof, floor, walls and windows of the sample building and Table 9 the overall heat transfer coefficient for the doors and windows.

TABLE 8: Total area of selected sample building

| Element | Area ($m^2$) |
|---|---|
| Roof | 106 |
| Floor | 106 |
| Walls | 385.2 |
| Windows | 33.6 |

TABLE 9: Overall heat transfer coefficient (W/°C $m^2$) for doors and windows

| Material | Door | Single glazing | Double glazing |
|---|---|---|---|
| Wood | 3.50 | 5.00 | 2.70 |
| Steel | 5.80 | 6.70 | 3.50 |
| Aluminium | 7.00 | 6.70 | 3.50 |

### 4.3.2 Building parameters

**Heat transfer coefficient.**
The heat transfer coefficient is a constant describing the heat transfer between the building and its environment due to conduction, convection and radiation heat loss. It is calculated under no insulation condition, according to the following formula:

$$U_{tatal} = \frac{U_1 A_1 + U_2 A_2 + \ldots}{A_{tatal}} \tag{26}$$

where $U_n$ = Heat transfer coefficient of different components constituting the building (walls, windows, ceilings and floors) (W/°C$m^2$);
$A_n$ = Surface area of each component ($m^2$);
$A_{total}$ = Total surface area of the building ($m^2$).

*Walls heat transfer coefficient:* Values for inside and outside surface film resistance are given in Tables 10 and 11. The walls total heat transfer coefficient is given in Table 12.

TABLE 10: General inside film resistance, $R_i$ (°C m$^2$ /W) for construction material

| Element | Heat direction | $R_i$ |
|---|---|---|
| Walls | Horizontal | 0.12 |
| Ceilings and floors | Upward | 0.10 |
| | Downward | 0.15 |

TABLE 11: General outside film resistance, $R_o$ (°C m$^2$ /W) for construction material for different wind speeds

| Wind speed (m/s) | ≤0.5 | 0.5-5.0 | ≥5.0 |
|---|---|---|---|
| Walls | 0.08 | 0.06 | 0.03 |
| Ceilings and floors | 0.07 | 0.04 | 0.02 |
| Exposed floors | 0.09 | - | - |

TABLE 12: External walls heat transfer coefficient for construction material

| | ***X*** **(m)** | ***k*** **(W/m°C)** | ***R*** **(°C m$^2$/W)** |
|---|---|---|---|
| Concrete | 0.02 | 1.21 | 0.017 |
| Brick | 0.2 | 0.6 | 0.333 |
| Stone | 0.02 | 2.27 | 0.009 |
| Chalk | 0.02 | 4.65 | 0.004 |
| $R_i$ | | | 0.120 |
| $R_o$ | | | 0.030 |
| $R_{total}$ | | | 0.496 |

Hence, $U_{wall} = 1/ R_{total} = 1/0.50 = 2$ W/°C m$^2$

*Roof heat transfer coefficient:* As for calculating the heat transfer coefficient for the roof, the construction materials for the roof are composed of two kinds, one is concrete and the other is hollow bricks. The concrete covers 80% of the total area, and the remainder is covered by hollow bricks. So, two kinds of heat transfer coefficient are calculated as follows, according to Tables 13 and 14:

TABLE 13: Roof's heat transfer coefficient for bricks

| | ***X*** **(m)** | ***k*** **(W/m°C)** | ***R*** **(°C m$^2$/W)** |
|---|---|---|---|
| Asphalt | 0.03 | 0.7 | 0.043 |
| Concrete | 0.02 | 1.75 | 0.011 |
| Reinforced concrete | 0.05 | 1.75 | 0.029 |
| Roof brick | 0.2 | 0.95 | 0.211 |
| Chalk | 0.015 | 4.65 | 0.0031 |
| $R_i$ | | | 0.100 |
| $R_o$ | | | 0.020 |
| $R_{total}$ | | | 0.417 |

Hence, $U_1 = 1 / R_{total} = 1/0.42 = 2.38$ W/°C m$^2$

TABLE 14: Roof's heat transfer coefficient for concrete

| | ***X*** **(m)** | ***k*** **(W/m°C)** | ***R*** **(°C m²/W)** |
|---|---|---|---|
| Asphalt | 0.03 | 0.7 | 0.043 |
| Concrete | 0.02 | 1.75 | 0.0113 |
| Reinforced concrete | 0.25 | 1.75 | 0.143 |
| Chalk | 0.015 | 4.65 | 0.0033 |
| $R_i$ | | | 0.100 |
| $R_o$ | | | 0.020 |
| $R_{total}$ | | | 0.320 |

And, $U_2 = 1 / R_{total} = 1/0.32 = 3.125$ W/°C m$^2$

Therefore, $U_{roof} = \dfrac{U_1 A_1 + U_2 A_2}{A_{total}} = 2.53$ W/°C m$^2$

*Floor heat transfer coefficient:* The floor's total heat transfer coefficient is given in Table 15.

TABLE 15: Floor heat transfer coefficient

| | ***X*** **(m)** | ***k*** **(W/m°C)** | ***R*** **(°Cm²/W)** |
|---|---|---|---|
| Sand | 0.07 | 0.38 | 0.184 |
| Concrete | 0.02 | 1.4 | 0.014 |
| Stone | 0.02 | 2.27 | 0.009 |
| $R_i$ | | | 0.150 |
| $R_o$ | | | 0.090 |
| $R_{total}$ | | | 0.448 |

And $U_{floor} = 1 / R_{floor} = 1/0.45 = 2.22$ W/°C m$^2$

*Windows:* As for windows, the type is single glass with a $U$ value of 6 W/℃ m$^2$

*Building total heat transfer coefficient:* After determining each part's heat transfer coefficient, the total building's heat transfer coefficient can be easily determined using Equation 26. The results are given in Table 16.

TABLE 16: Building's total heat transfer coefficient

| **Surface** | ***U*** **(W/m²°C)** | ***A*** **(m²)** | ***UA*** **(W/°C)** |
|---|---|---|---|
| Roof | 2.53 | 212.0 | 536.36 |
| Floor | 2.22 | 212.0 | 470.64 |
| External walls | 2.00 | 499.2 | 998.40 |
| Windows | 6.00 | 67.2 | 403.20 |
| Total | | 990.4 | 2408.60 |

And hence, $U_{total} = 2408.6 / 990.4 = 2.43$ W/°C m$^2$.

**Building's thermal mass (*C*).**
Thermal mass is the ability of a building to store heat. It is the second parameter needed for simulation.

*The heat transfer through walls*: There is a temperature gradient through the wall layers, with the lowest temperature at the layer adjacent to the outside. So the concept of efficient thermal mass is defined by which part of the wall that can store heat for the indoor temperature of 20℃. Figure 11 shows the heat transfer through composite walls. The theoretical equation for calculations is given in Equation 27, but Equation 28 gives a simplified one, used for practical calculations:

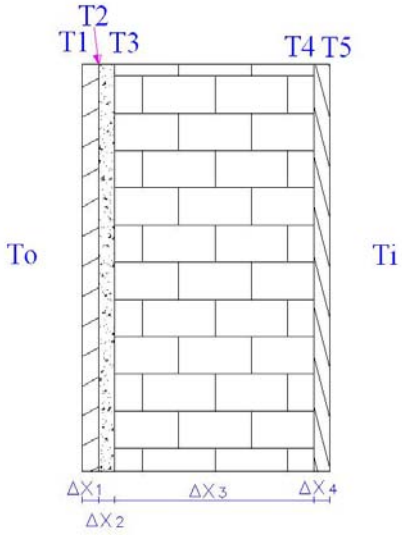


FIGURE 11: Heat transfer through composite walls

$$\frac{E}{A} = \int_0^s (T_x - T_0) c_p(x) \rho(x) dx = \int_0^s (T_i - T_0) c_p(x) \rho(x) dx \qquad (27)$$

where $E$ = Wall thermal energy (J);
$A$ = Wall area ($m^2$);
$S$ = Wall thickness (m);
$T_x$ = Material's mean temperature (°C);
$T_i$ = Indoor temperature (°C);
$T_o$ = Outdoor temperature (°C);
$c_p$ = Material's specific heat (kJ/kg °C);
$\rho$ = Material's density ($kg/m^3$).

For our case, Equation 27 becomes (see Figure 11):

$$Q = \frac{T_o - T_1}{R_o} = \frac{T_1 - T_2}{R_1} = \frac{T_2 - T_3}{R_2} = \frac{T_3 - T_4}{R_3} = \frac{T_4 - T_5}{R_4} = \frac{T_5 - T_i}{Ri} \qquad (28)$$

Equation 28 can be solved giving the following (Figure 12):

$T_i$ = 20°C
$T_o$ = −5°C
$Q$ = 50.71 W
$T_1$ = −3.48°C
$T_2$ = −3.03°C
$T_3$ = −2.19°C
$T_4$ = 14.71°C
$T_5$ = 14.93°C

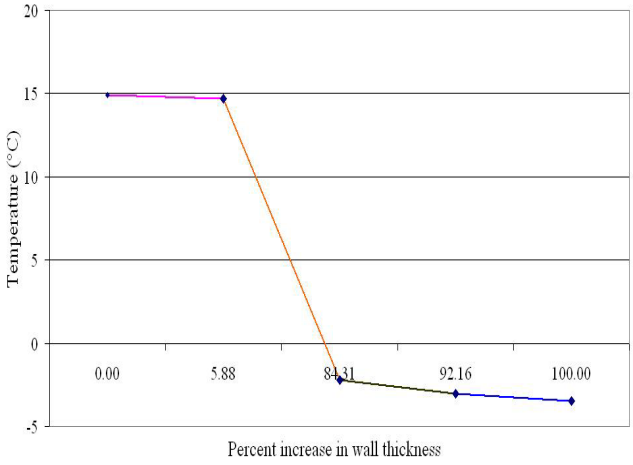


FIGURE 12: Temperature gradient through walls

Then the mean temperature of each layer is found, subtracted from the outdoor temperature and then multiplied by that material's thermal capacity and density to get the results shown in Table 17.

TABLE 17: Walls thermal capacity

| | $T_m$ (°C) | $T_o$ (°C) | $T_m$-$T_o$ (°C) | $x$ (m) | Area (m²) | Density (kg/m³) | Specific heat (kJ/(kg°C)) | $C$ (kJ/°C) |
|---|---|---|---|---|---|---|---|---|
| Stone | -3.26 | -5.00 | 1.74 | 0.02 | 499.20 | 2580.00 | 0.88 | 39550 |
| Concrete | -2.61 | -5.00 | 2.39 | 0.02 | 499.20 | 2088.00 | 1.08 | 53748 |
| Brick | 6.26 | -5.00 | 11.26 | 0.20 | 499.20 | 1400.00 | 1.08 | 1699564 |
| Chalk | 14.82 | -5.00 | 19.82 | 0.02 | 499.20 | 2710.00 | 0.86 | 345884 |

Table 18 shows the wall's equivalent thermal capacity, Table 19 the thermal mass of the external walls and Table 20 the thermal mass for the internal walls.

TABLE 18: Walls equivalent thermal capacity

| | $T_m$-$T_o$ (°C) | $X$ (m) | Area (m²) | Density (kg/m³) | Specific heat (kJ/(kg°C)) | $C$ (kJ/°C) |
|---|---|---|---|---|---|---|
| Bricks | 25 | 0.2 | 499.2 | 1400.00 | 1.08 | 3773952 |
| Chalk | 25 | 0.015 | 499.2 | 2710.00 | 0.86 | 436288 |

TABLE 19: External walls thermal mass

| | $X$ (m) | Area (m²) | Density (kg/m³) | Specific heat (kJ/(kg°C)) | $C$ (kJ/°C) |
|---|---|---|---|---|---|
| Bricks | 0.20 | 499.20 | 1400.00 | 1.08 | 150958 |
| Chalk | 0.015 | 499.20 | 2710.00 | 0.86 | 17452 |
| $C_{total}$ | | | | | 168410 |

TABLE 20: Internal walls thermal mass (bricks walls)

| | $X$ (m) | Area (m²) | Density (kg/m³) | Specific heat (kJ/(kg°C)) | $C$ (kJ/°C) |
|---|---|---|---|---|---|
| Chalk | 0.015 | 271.2 | 2710 | 0.86 | 9481 |
| Brick | 0.1 | 271.2 | 1400.00 | 1.08 | 41005 |
| Chalk | 0.015 | 271.2 | 2710 | 0.86 | 50486 |
| $C_{total}$ | | | | | 100972 |

Tables 21-23 show the results of calculation of thermal mass of floor and roof.

TABLE 21: Thermal mass of floor

| | $X$ (m) | Area (m²) | Density (kg/m³) | Specific heat (kJ/(kg°C)) | $C$ (kJ/°C) |
|---|---|---|---|---|---|
| Concrete | 0.015 | 212 | 2088.00 | 1.08 | 7171 |
| Stone | 0.02 | 212 | 2580.00 | 0.88 | 9627 |
| $C_{total}$ | | | | | 16798 |

TABLE 22: Thermal mass of roof (with bricks)

| | $X$ (m) | Area (m²) | Density (kg/m³) | Specific heat (kJ/(kg°C)) | $C$ (kJ/°C) |
|---|---|---|---|---|---|
| Brick | 0.2 | 169.6 | 1400.00 | 1.08 | 51287 |
| Chalk | 0.015 | 169.6 | 2710.00 | 0.86 | 5929 |
| $C_{total}$ | | | | | 57216 |

TABLE 23: Thermal mass of roof (without bricks)

| | ***X*** **(m)** | **Area (m²)** | **Density (kg/m³)** | **Specific heat (kJ/(kg°C))** | ***C*** **(kJ/°C)** |
|---|---|---|---|---|---|
| Concrete | 0.25 | 42.4 | 2088.00 | 1.08 | 23904 |
| Chalk | 0.015 | 42.4 | 2710 | 0.86 | 1482 |
| $C_{total}$ | | | | | 25386 |

Hence, the total thermal mass of the roof becomes: $C_{roof}$ = 57216 + 25386 = 82602 kJ/℃

Table 24 summarizes the calculations of the thermal mass of the building.

TABLE 24: The total thermal mass of the building

| **Surface** | ***C*** **(kJ/°C)** |
|---|---|
| Roof | 82602 |
| Floor | 16798 |
| External walls | 168410 |
| Internal walls | 100973 |
| Total | 368782 |

### 4.4 Building heat load models

According to Valdimarsson (1993), simulation models for district heating systems are made to describe time dependent behaviour of the system. Many types of models exist, and they have different scale for simulations. Models of district heating systems can be classified as follows:

- By type - microscopic or macroscopic;
- By method - dynamic or steady-state;
- By approach - physical or black box;
- By usage - design or operation.

The signals encountered in district heating systems are summarized in Table 25.

TABLE 25: Main influencing signals in the simulation of district heating systems

| **Input signals** | **Control signals** | **State signals** | **Output signals** |
|---|---|---|---|
| Outdoor temperature | System water supply temperature | Indoor temperature | Water flow |
| Wind velocity | Water pressure | Water quantity in storage | Return water temperature |
| Wind direction | | | System heat load |
| Solar radiation | | | |
| Cloud coverage | | | |

In this section, models for district heating networks are described. Models in this work are macroscopic physical models. The district heating network is lumped into one model block. The whole system is modelled as seen from the district heating water supply station. Most variables for the theory of heat load models are defined in the Nomenclature.

The lumped heat capacity model analyzing systems may be considered uniform in temperature. The lumped heat capacity analysis is one which assumes that the internal resistance of the body is

negligible in comparison with the external resistance. So, the temperature of the body is only the function of time, which has nothing to do with coordinates. It seems that all the quality and heat capacity of the body concentrate on the one particle. The following formula is given according to the above assumption.

$$Q = hA(T - T_\infty) = -C\frac{dT}{dt} \tag{29}$$

where $A$ = The surface area for convection ($m^2$);
$C$ = Heat capacity (kJ/°C).

### 4.4.1 Radiators

For heat transfer from the heating system to the heated place, a heat exchanger is used, which is a known radiator. According to Anon (1977), the relative heat load of a radiator can be written as:

$$\frac{Q}{Q_0} = \left(\frac{\Delta T_m}{\Delta T_{m0}}\right)^{(4/3)} = \left(\frac{T_s - T_r}{\ln\left(\frac{T_s - T_i}{T_r - T_i}\right)} \cdot \frac{\ln\left(\frac{T_{s0} - T_{i0}}{T_{r0} - T_{i0}}\right)}{T_{s0} - T_{r0}}\right)^{(4/3)} \tag{30}$$

where $Q/Q_0$ = Ratio of the actual heat output from the radiator to the heat output at design conditions;
$T_s$ = Water supply temperature (°C);
$T_r$ = Water return temperature (°C);
$T_i$ = Room temperature (°C).

The logarithmic temperature difference, $\Delta T_m$, for radiators is defined as:

$$\Delta T_m = \frac{(T_s - T_i) - (T_r - T_i)}{In\frac{T_s - T_i}{T_r - T_i}} = \frac{(T_s - T_r)}{\ln(\frac{T_s - T_i}{T_r - T_i})} \tag{31}$$

### 4.4.2 Water heat duty

When the hot water in the district heating system is going through the radiators, it gives the heat load. According to Valdimarsson (2003), this value is given as:

$$Q = C_p m(T_s - T_r) \tag{32}$$

The relative heat load of water flow can be written as:

$$\frac{Q}{Q_0} = \frac{m(T_s - T_r)}{m_0(T_{s0} - T_{r0)}} \tag{33}$$

### 4.4.3 Building heat loss

Heat loss through the building can be calculated with Equation 34:

$$Q_{loss} = k_l(T_i - T_o) \tag{34}$$

where $k_l$ = Building heat loss factor, which is a constant.

Relative heat loss can be obtained as:

$$\frac{Q_{loss}}{Q_{loss0}} = \frac{T_i - T_o}{T_{io} - T_{oo}} \tag{35}$$

### 4.4.4 Pipe heat loss

In the district heating system, there is heat loss through the pipes between the pumping station and the buildings to be heated. This value of heat loss can be calculated by using the district heating pipe transmission effectiveness parameter. According to Valdimarsson (1993), the transmission effectiveness $\tau$ is defined as follows:

$$\tau = \frac{T_s - T_g}{T_1 - T_g} = e^{\frac{U_p}{mc_p}} \tag{36}$$

The reference value $\tau_o$ can be concluded from the reference flow conditions:

$$\tau_o = \frac{T_{so} - T_g}{T_{1o} - T_g} = e^{\frac{U_p}{m_o c_p}} \tag{37}$$

Parameters $U_p$ and $c_p$ are assumed to be constant all over the system. By combining Equations 36 and 37, the transmission effectiveness can be obtained:

$$\tau = \tau_o^{\frac{m_m}{m}} \tag{38}$$

By combining Equations 36 and 38, the supply temperature to the house can be calculated:

$$T_s = T_g + (T_1 - T_g)\tau = T_g + (T_1 - T_g)\tau_o^{\frac{m_o}{m}} \tag{39}$$

If the district heating network circulates water, the return water temperature at the pumping station is obtained from Equation 40:

$$T_2 = T_g + (T_r - T_g)\tau = T_g + (T_r - T_g)\tau_o^{\frac{m_o}{m}} \tag{40}$$

### 4.4.5 Building energy storage

When the heating of a building is turned of, the building does not cool down immediately. The building has heat capacity and it stores energy. The building energy storage model is given by:

$$\frac{dT_i}{dt} = \frac{1}{C}Q_{net} = \frac{1}{C}(Q_{supp} - Q_{loss)} = \frac{1}{C}(mc_p(T_s - T_r) - k_l(T_i - T_o)) \tag{41}$$

In a steady-state model, all time derivatives equal to zero, but in a dynamic model these parameters are effective.

### 4.5 Steady-state approach

When steady-state conditions are assumed to be established in the district heating system, heat is not to be stored in the buildings. Return temperature $T_r$ can be calculated by combining Equations 34 and 36 (see Nappa, 2000):

$$\frac{Q}{Q_0} = \left( \frac{T_s - T_r}{T_{s0} - T_{r0}} \cdot \frac{\ln\left(\frac{T_{s0} - T_{i0}}{T_{r0} - T_{i0}}\right)}{\ln\left(\frac{T_s - T_i}{T_r - T_i}\right)} \right)^{4/3} = \frac{T_i - T_o}{T_{io} - T_{oo}} \tag{42}$$

$T_r$ can be calculated with iteration from Equation 43. According to Valdimarsson (1993), the fastest convergence is obtained, when $T_r$ inside logarithm is calculated:

$$T_{r,n+1} = (T_s - T_i)e^{-z} + T_i \tag{43}$$

Here $z$ is defined as:

$$z = \frac{T_s - T_{r,n}}{T_{so} - T_{ro}} \left( \frac{T_{io} - T_{oo}}{T_i - T_o} \right)^{3/4} \ln\left( \frac{T_{so} - T_{io}}{T_{ro} - T_{io}} \right) \tag{44}$$

With outside temperature data known, $T_i$ assumed to be constant, and the supply temperature known, $T_{r,n+1}$ can be found iteratively from Equation 43.

In the steady-state model, the heat loss from buildings is the same as the heat load supply:

$$Q_{supp} = Q_{loss} \tag{45}$$

or

$$mc_p(T_s - T_r) = k_l(T_i - T_o) \tag{46}$$

The mass flow is obtained directly from Equation 46 as:

$$m = \frac{k_l(T_i - T_o)}{c_p(T_s - T_r)} \tag{47}$$

with the factor $k_l$ calculated from the reference conditions:

$$k_l = \frac{m_o c_p(T_{so} - T_{ro})}{T_{io} - T_{oo}} \tag{48}$$

### 4.6 Reference values and constants

All reference values are here marked with the subscript *o*. Common reference values for geothermal district heating networks are:

| | |
|---|---|
| Supply water temperature | $T_{so}$ = 80°C; |
| Return water temperature | $T_{ro}$ = 35°C; |
| Room temperature | $T_{io}$ = 20 °C; |

Similar reference values used for fuel fired networks are:

| | |
|---|---|
| Supply water temperature | $T_{so} = 90°C$; |
| Return water temperature | $T_{ro} = 65°C$; |
| Room temperature | $T_{io} = 20°C$; |

The reference value for the outside temperature depends on the climate. The reference value for the Moeil village $T_{oo} = -5°C$ was used here for both the geothermal and the fuel-fired systems. Ground temperature was assumed to be constant at 7°C. The reference mass flow of water is related to the size of network to be studied. Here it was selected to be 0.32 kg/s. The specific heat capacity of water $c_p$ = 4.186 (kJ/ (kg°C), is assumed to be constant and dependence of temperature was neglected.

### 4.7 Simulation results - geothermal system

The steady-state model described in Section 4.5 was programmed with MATLAB with reference to the weather data presented in Section 4.1. The results are presented in Figures 13-18.

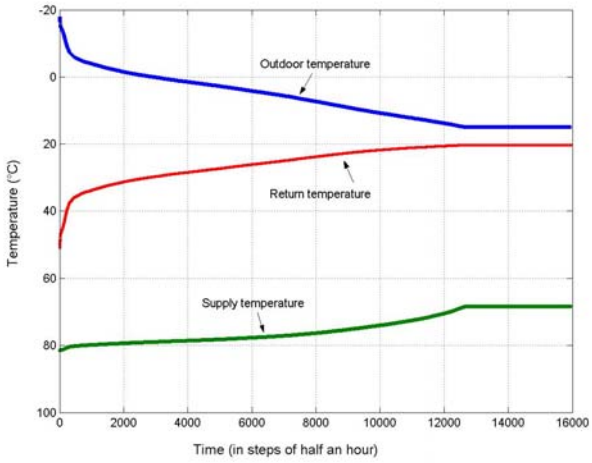


FIGURE 13: Duration curve of supply, return and outdoor temperature

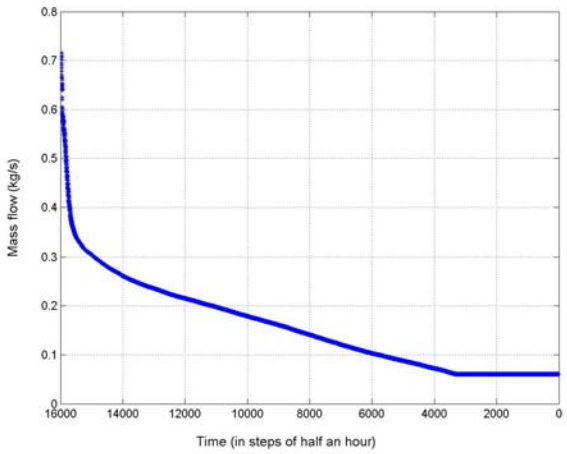


FIGURE 14: Duration curve of mass flow

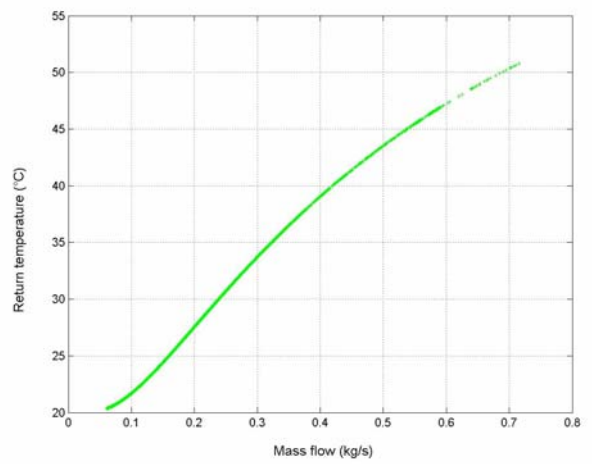


FIGURE 15: Return temperature as a function of mass flow

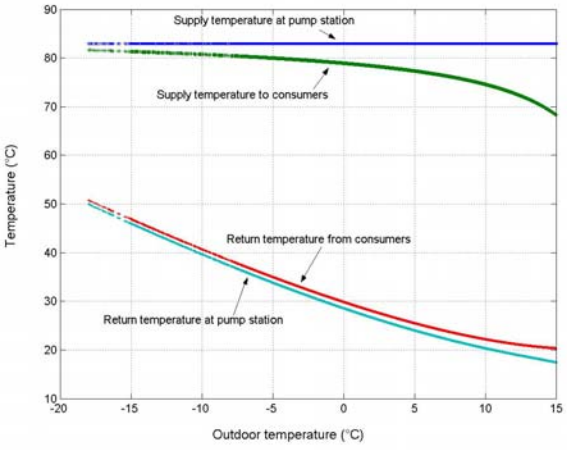


FIGURE 16: Water temperature in different positions of the network

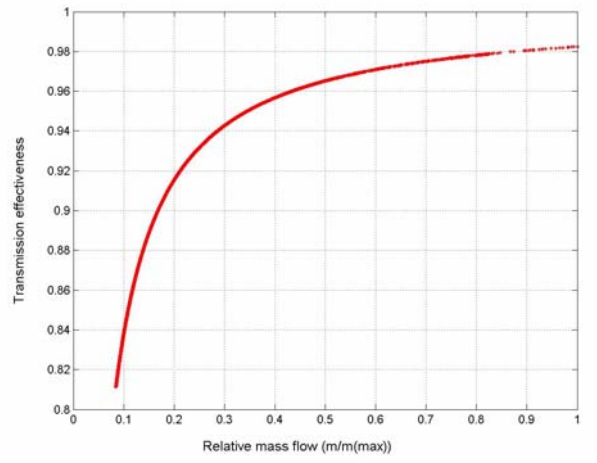


FIGURE 17: Pipe transmission effectiveness as a function of relative mass flow

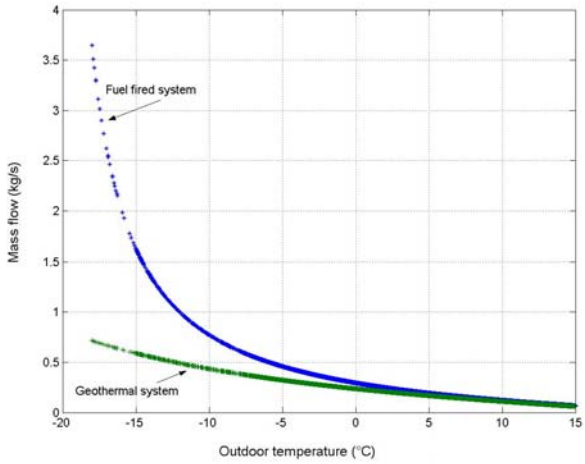


FIGURE 18: Comparison of mass flow for the two heating systems

Results analysis:

1. Figure 13 shows the duration curve for outdoor temperature $T_o$, return temperature $T_r$ and supply temperature $T_s$ during one year (per half an hour). It is necessary to mention that all calculations were done in the Matlab program. Outdoor temperatures of more than 15°C were assumed to be 15°C as no heat is required under these conditions. In this figure, the Y-axis is reversed.
2. The mass flow duration curve is shown in Figure 14. There are 22 days per year with higher mass flow than assumed available. The system will not be able to supply the required head during those 22 days, if such limitation is imposed. An economical analysis is due here to find the best value of such limit, considering cost of lack of heat versus the investment for additional wells.
3. Figure 15 shows the relationship between return temperature and mass flow. From this curve it can be seen that when mass flow increases, the return temperature also becomes higher. This means that most of the mass flow in the system has higher return temperature, as shown in Table 26. This is because when there is more heat requirement in the building (lower outdoor temperature), hot water circulation through the radiators will be increased (higher mass flow), and the temperature difference between the supply and return temperature will be smaller.
4. Figure 16 shows the water temperature in the district heating network. The water temperature at pump station ($T_1$), supply temperature to consumers ($T_s$), return temperature from consumer and return temperature to pump station ($T_2$). Temperature difference between $T_r$ and $T_2$ shows heat loss through the pipe line. It is interesting to notice that when heat requirement is low, mass flow is low, so temperature drops in both the supply and return hot water will be high. Some critical temperatures are given in Table 26.
5. Figure 17 shows the pipe transmission effectiveness $\tau$, as a function of relative mass flow ($m/m_{max}$).
6. Figure 18 finally shows the relationship between outdoor temperature and mass flow for typical geothermal and fossil fuel fired systems A typical geothermal system is taken to have 80/35°C design temperatures for supply and return, whereas a typical fuel fired system has 90/65°C as design temperatures. The geothermal system will require larger radiators, in order to obtain these design temperature. This investment is justified by less mass flow required from the wells. Else more wells will have to be drilled and the yearly utilization time of these additional wells will be low.

TABLE 26: Maximum and minimum parameters in the geothermal district heating system

| | $T_o$ (°C) | $T_1$ (°C) | $T_2$ (°C) | $T_r$ (°C) | $T_s$ (°C) | $m$ (°C) | $Q$ (kW) | ΔT | $T_s$-$T_r$ (°C) | $T_r$-$T_2$ (°C) |
|---|---|---|---|---|---|---|---|---|---|---|
| Maximum | 15 | 83 | 49.98 | 50.78 | 81.63 | 0.72 | 92.34 | Minimum | 30.85 | 0.80 |
| Minimum | -18 | 83 | 17.45 | 20.35 | 68.29 | 0.06 | 12.15 | Maximum | 47.79 | 2.90 |

### 4.8 Network calculation

The network calculation involves finding the system parameters in such a way, that a predefined cost function has a minimum. A scheme of the network is shown in Figure 19.

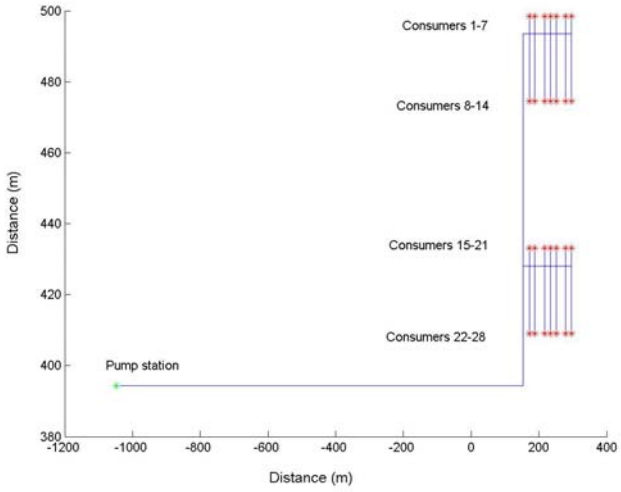


FIGURE 19: Scheme of network

#### 4.8.1 Pipe

The pipes have a resistance defined by the Darcy-Weisbach equation, which is written as:

$$h = \frac{v^2}{2g}\frac{L}{D}f = \frac{8m^2 Lf}{D^2\rho^2\pi^2 g} \qquad (49)$$

The friction factor $f$ can be calculated from the Colebrook - White equation:

$$\frac{1}{\sqrt{f}} = \left(\frac{a}{\mathrm{Re}\sqrt{f}} + \frac{b}{kD}\right)^2 \qquad (50)$$

#### 4.8.2 Nodal pressure

The pressure at the nodes is determined by the element pressure loss. If a target pressure loss per unit length is defined, a target nodal pressure is also defined. The voltage law of Kirchhoff places restrictions on this, because the pressure loss along any closed path has to sum up to zero, and makes it therefore impossible to obtain target pressure loss in all the elements. A loop free network has a unique solution for the nodal pressure.

#### 4.8.3 The least squares *dP/L* solution of nodal pressure

If the nodal pressure is considered an independent variable, the pressure loss per unit length can be calculated for all elements (Valdimarsson, 2001).

In this paper, we focus on a network with a total pipe length of 3.82 km and serving 28 buildings. So-called *h/L* diagrams are presented here to show the network performance. On these diagrams, the nodal head is plotted as a function of the distance from the inlet point, measured according to a selected tree set. Thus, one pipe in each loop, the link, is not represented with correct length. The *h/L* diagram for the existing network is shown in Figure 20 and shows the pressure drop per node of network. The network shown is the supply network with a total pipe length of 3.82 km. The return network has a similar topology but opposite flow direction, and is not treated in this paper.

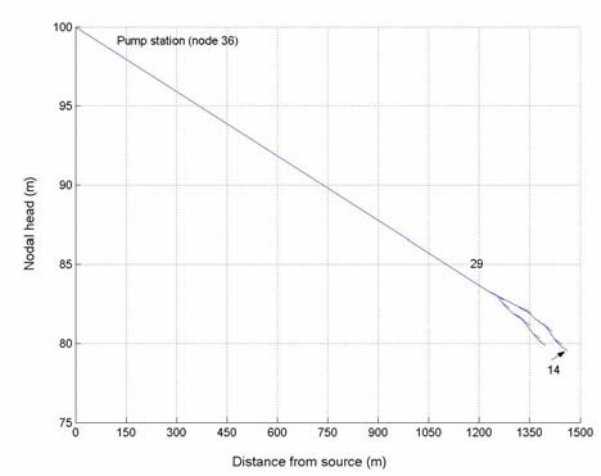


FIGURE 20: Pressure drop in the network

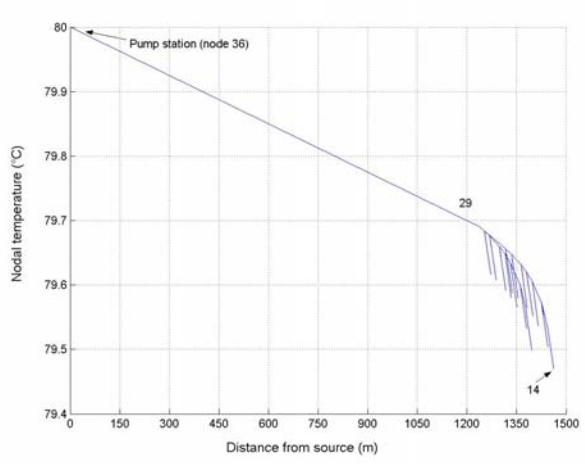


FIGURE 21: Temperature drop in the network

Figure 21 shows the temperature drop per node of network. From Table 27 it can be seen that the results are reasonable.

TABLE 27: Maximum and minimum values for pressure and temperature drops

| Parameters | Maximum (node 36) | Minimum (node 14) | Peak value (pipe 36-29) |
|---|---|---|---|
| Head drop (m) | 100 | 79.55 | 16.32 |
| Temperature (°C) | 80 | 79.47 | 0.30 |

## 5. CONCLUSIONS

The main conclusions derived from this work are summarized as follows:

1) The swimming pool is designed according to the most common standards regarding the required dimensions and sanitary equipment. The surface area of the pool is designed as 412.5 $m^2$ and to keep the pool water temperature at 27°C at -5°C outdoor temperature, a heating capacity of 711 kW is needed.
2) The artesian hot water spring available in the Sabalan geothermal area, Gheynarjeh with a flow rate of 7 l/s, at temperature of 83°C, can be used as a heat source for a swimming pool. According to the calculations performed in the project, 4.25 l/s of 75°C hot water are required for this purpose.
3) A steady-state model for both a geothermal district heating system and a fuel-fired system has been developed and the relationship between outdoor temperature and mass flow in both of them compared. In the geothermal heating system, the mass flow is lower and the radiators larger, so it is both possible and favourable from an economical point of view.
4) The heating has a sharp peak load, so limitation of the maximum flow may be cost-effective compared to drilling additional geothermal wells with low utilization time.
5) A simulation model is a powerful tool for studying and analyzing district heating systems.
6) Maximum mass flow and radiator sizes are important parameters affecting the indoor temperature of district heating systems. The maximum mass flow can be controlled by a control valve.
7) In the long run, it can be economically advantageous to pay more attention to insulation of buildings and their energy storage ability in Iran. This is based on present condition of buildings and energy costs in the country.
8) In this paper, geothermal utilization in the Sabalan geothermal area in NW-Iran was discussed. It is necessary to study detailed technical solutions and economic feasibility before real systems are set up.

**ACKNOWLEDGEMENTS**

I would like to express my gratitude to Dr. Ingvar Birgir Fridleifsson, director, and Mr. Lúdvík S. Georgsson, deputy director, of the UNU Geothermal Training Programme for their hospitality and selfless dedication to the UNU Fellows. My deepest thanks to Mrs. Gudrún Bjarnadóttir for her efficient help and kindness before and during the whole training period. I am also thankful to SUNA - Iran for supporting me during these 6 months. I especially want to extend my unreserved gratitude to my supervisor Professor Páll Valdimarsson, for his excellent technical support, lectures and friendliness. At the same time, I am grateful to my second supervisor Dr. Árni Ragnarsson who shared his deep knowledge and gave me opportunity to meet with the following experts; Thorlákur Jónsson from Almenna Consulting Engineers Ltd. and Kristján Thór Hálfdánarson from VST Consulting Engineers Ltd. to whom I owe a lot of gratitude.

Additionally, I would like to thank all the lecturers and the staff members at Orkustofnun and ISOR for the knowledge and assistance given to us during the lecture sessions. I also thank the UNU Fellows of 2004 for their unforgettable friendship and cooperation during our training time, especially the engineering group and in particular Miss Lei Hayan for her help in this work.

Finally, my deepest thanks to my family for their moral support during the six months. I dedicate this work to members of my family and friends who gave me spiritual inspiration during my stay in Iceland. I say thank you so much and god bless you all.

**NOMENCLATURE**

| | | |
|---|---|---|
| $A$ | = | Heat transfer area ($m^2$); |
| $C$ | = | Heat capacity of building (kJ/°C); |
| $U$ | = | Heat transfer coefficient ($W/m^2$ °C); |
| $c_p$ | = | Water heat capacity (kJ/kg °C); |
| $Q$ | = | Heat load (W); |
| $Q_{supp}$ | = | Heat supply (W); |
| $Q_{loss}$ | = | Heat loss (W); |
| $T_w$ | = | Wall surface temperature (°C) ; |
| $T_i$ | = | Indoor temperature (°C); |
| $T_o$ | = | Outdoor design temperature (°C); |
| $T_1$ | = | Pipe inlet temperature (°C); |
| $T_2$ | = | Return temperature at pumping station (°C); |
| $T_{io}$ | = | Reference indoor temperature (°C); |
| $T_{oo}$ | = | Reference outdoor temperature (°C); |
| $T_{so}$ | = | Reference supply temperature (°C); |
| $T_{ro}$ | = | Reference return temperature (°C); |
| $T_s$ | = | Water supply temperature (°C); |
| $T_r$ | = | Water return temperature (°C); |
| $T_{c1}$ | = | Cold fluid inlet temperature (°C); |
| $T_{c2}$ | = | Cold fluid outlet temperature (°C); |
| $T_g$ | = | Ground temperature (°C); |
| $\Delta T_m$ | = | Logarithmic mean temperature difference (°C); |
| $\Delta T_{mo}$ | = | Logarithmic mean temperature difference at reference conditions (°C); |
| g | = | Acceleration due to gravity ($m/s^2$) |
| $k_l$ | = | Building heat loss factor (kW/°C); |
| $m$ | = | Water mass flow (kg/s); |
| $m_{ave}$ | = | Average mass flow (kg/s); |
| $\tau$ | = | Pipe transmission effectiveness. |

## REFERENCES

Anon, 1977: *DIN 4703 Teil 3. Varmeleistung von Raumheizkörper* (in German). Beuth Verlag, Berlin, Germany.

Bogie, I., Cartwright, A.J., Khosrawi, K., Talebi, B., and Sahabi, F., 2000: The Meshkin Shahr geothermal prospect, Iran. *Proceedings of the World Geothermal Congress 2000, Kyushu-Tohoku, Japan, 997-1002*.

Bromley, C., Khosrawi, K., and Talebi, B., 2000: Geophysical exploration of Sabalan geothermal prospect in Iran. *Proceedings of the World Geothermal Congress 2000, Kyushu-Tohoku, Japan, 1009-1014*.

Emeish, M.E., 2001: *Simulation of heating systems in Jordanian buildings*. University of Iceland, M.Sc. thesis, UNU-GTP, Iceland, report 1, 91 pp.

Fotouhi, M., 1995: Geothermal development in Sabalan, Iran. *Proceedings of the World Geothermal Congress 1995, Florence, Italy, 1,* 191-196.

Khosrawi, K., 1996: Geochemistry of geothermal springs in the Sabalan area, Azarbydjan-Iran. Report 7 in: *Geothermal Training in Iceland 1996*. UNU-GTP, Iceland, 135-159.

Nappa, M., 2000: *District heating modelling*. University of Iceland, report, 47 pp.

Noorollahi, Y., and Yousefi Sahzabi, H., 2003: Preliminary Environmental Impact Assessment of a geothermal project in Meshkin Shahr, NW-Iran. *Proceedings of the International Geothermal Conference IGC2003, Multiple integrated uses of geothermal resources, Reykjavik*, S12, 1-11.

Olson, R.M., 1973: *Essentials of engineering fluid mechanics*. Intext Educational Publishers, New York, 637 pp.

Perkins, P.H., 1988: *Swimming pool*. Elsevier Applied Science Ltd., London, 359 pp.

Pool Warehouse, 2004: *Inground swimming pools and spas*, Pool Warehouse web page, http://www.poolwarehouse.com.

Pump-flo.com, 2004: *Experience internet pump selection*. Web page, http://www.pump-flo.com.

Rensselaer, 2004: *Teaching archive for biochemical engineering and environmental engineering.* Rensselaer Web page, http://www.rpi.edu/dept/chem-eng/Biotech-Environ/COAG/home.htm.

Sahabi, F., Khoshlessan, M.R., and Barnett, P.R, 1999: Geothermal exploration of Mt. Sabalan, NW Iran. *Geothermal Resources Council, Transactions, 23*, 479-484.

Svavarsson, G., 1990: *Designing swimming pools*. University of Iceland, B.Sc. thesis (in Icelandic), 52 pp.

Valdimarsson, P., 1993: *Modelling of geothermal district heating systems.* University of Iceland, Ph.D. thesis, 144 pp.

Valdimarsson, P., 2001: *Pipe network diameter optimisation by graph theory*. Water Software Systems: Theory and applications, 1, 13 pp.

Valdimarsson, P., 2003: *District heating systems: Fundamentals and application.* Paper presented at 6th National Heating, Ventilating, Air-Conditioning and Sanitary Congress and Exhibition, Turkey.

Wark, K., 1988: *Thermodynamics*. McGraw-Hill Book Company, New York, 954 pp.

Yousefi Sahzabi, H., 2004: Application of GIS in the Environmental Impact Assessment of Sabalan geothermal field, NW-Iran. Report 19 in: *Geothermal training in Iceland 2004.* UNU-GTP, Iceland, 439-474.